Water Air Soil Pollut (2014) 225:1835
DOI 10.1007/s11270-013-1835-3

Pilot-Scale Test for a Phosphate Treatment Using Sulfate-Coated Zeolite at a Sewage Disposal Facility

Jae-Woo Choi · Kyu-Sang Kwon · Soonjae Lee · Byungryul An · Seok-Won Hong · Sang-Hyup Lee

Received: 10 October 2013 / Accepted: 4 December 2013 / Published online: 11 January 2014

Abstract The objective of this research was to evaluate a zeolite ball coated with sulfate (ZBCS) for the removal of phosphate in a batch, lab-scale column, and pilot-scale plant. Phosphate adsorption in the batch studies satisfactorily fitted to the Langmuir isotherm with a maximum adsorption capacity of 15.13 mg/g and the pseudo-first-order model with the amount of phosphate sorbed at equilibrium of 6.98 mg/g. The breakthrough data were satisfactorily described using the empirical model by Thomas. Phosphate adsorbed on the ZBCS was effectively desorbed using 10 % sulfuric acid and the surface-modified mineral was regenerated as an adsorbent for thrice adsorption and desorption cycles by maintaining the adsorption capacity at the value before regeneration. In addition, since the regeneration solution used for recycling of the ZBCS in the pilot plant is enriched with sulfate ion, the enriched solution could be used for resource recovery by various methods, such as mineral-based and chemical-based methods. Our research suggests a complete system for removal and recovery of phosphate from sewage and wastewater using a novel adsorbent based on minerals.

J.-W. Choi · K.-S. Kwon · S. Lee · B. An · S.-W. Hong · S.-H. Lee (✉)
Center for Water Resource Cycle Research, Korea Institute of Science and Technology, Hwarangno 14-gil 5, Seongbuk-gu, Seoul 136-791, Republic of Korea
e-mail: yisanghyup@kist.re.kr

S.-H. Lee
Graduate School of Convergence Green Technology and Policy, Korea University, Seoul 136-701, Republic of Korea

Keywords Zeolite · Sewage · Sulfate · Phosphate · Pilot plant

1 Introduction

Phosphorus compounds are an essential nutrient in the aquatic environment and are also widely used in detergents, pesticides, toothpaste, and nerve agents. The most important commercial exploitation of phosphorus is the production of fertilizer. In its natural state, phosphorus cannot be encountered in pure form, but only as phosphate, which consists of a phosphorus atom bonded to four oxygen atoms as a negatively charged ion. An immoderate concentration of phosphate as a nutrient is responsible for eutrophication, leading to environmental problems in reservoirs and coastal areas (Benyoucef and Amrani 2011). For this reason, phosphate removal during the sewage treatment process has become an essential research area for preventing algal blooms.

Removal technologies for phosphate have been investigated through physical, chemical, and biological processes including ion exchange (Blaney et al. 2007; Kim et al. 2012), chemical precipitation (Simmons 2010), coagulation (Jiang and Graham 1998), and biological methods (Oehmen et al. 2007). However, the chemical and biological processes among these technologies entail the problem of disposal of large volumes of waste sludge and their removal efficiency does not exceed approximately 30 % (Li et al. 2003; Choi et al. 2012). In contrast, adsorption and ion exchange are promising due to their simplicity, cost-effectiveness, efficiency, and potential for reuse (Boyer et al. 2011;

Low et al. 2011; Mohammed et al. 2011). Therefore, various adsorbents, such as apatite, clinoptilolite, alunite, and polymeric ion exchanger, have been applied for removal of phosphate (Ozacar 2003; Kandah 2004; Tillman et al. 2005).

Zeolite is porous crystalline aluminosilicate comprised of assemblies of SiO_4 and AlO_4. The general stoichiometric unit formula for a zeolite is $M_{x/m}[(AlO_2)_x(SiO_2)_y]$ zH_2O, where M is the cation with valence m, z is the number of water molecules in each unit, and x and y are integers such that y/x is greater than or equal to 1 (Dionisiou et al. 2013). To activate the zeolite, the water molecules are removed by raising the temperature or pulling a vacuum. This results in a framework with the remaining atoms intact and the material is filled with cavities connected by pores. In addition, the Si/Al ratio can be adjusted. Thus, zeolites with widely different adsorptive properties may be tailored by the appropriate choice of framework structure, cationic form, and Si/Al ratio to achieve the selectivity required for a given separation objective (Celik et al. 2010). The ionic property of zeolite means that it has a high affinity for various polar molecules such as water and hydrogen sulfide. On the other hand, the zeolite has hydrophobicity as the Si/Al ratio is increased. For this reason, some zeolites can be used for the removal of volatile organic compounds (Motsa et al. 2012). Meanwhile, various functionalization studies have been conducted to investigate enhancing the adsorption capacity and the selectivity of adsorbents (Aguado et al. 2009; Zaib et al. 2012; Felice et al. 2013; Liang et al. 2013). The advantages of surface modification as a functionalization are its simplicity, flexibility, and broad variety of possible functional groups that can be applied to the surface of adsorbents.

The aim of the present research is to investigate and model the removal of phosphate from real sewage employing a sulfate-coated zeolite in a batch, a fixed-bed column in a laboratory, and a pilot system in a sewage treatment plant. The empirical models of Adams-Bohart and Thomas are used to describe the data of the column and pilot-scale experiments. The important parameters related to an optimal design of a pilot plant, such as bed height, flow rate, and initial phosphate concentration have been investigated. A study was also conducted to develop a suitable technique to regenerate the adsorbent for reuse, as well as for the recovery of the desorbed phosphate for economic benefit.

2 Materials and Methods

2.1 Chemical

The zeolite powder (clinoptilonite; $(Na_2Ca)(Al_2SiO_{18})\cdot 6H_2O$) and sulfuric acid (98 %) used in this research were obtained from Sigma-Aldrich (Yong-In, Korea). The phosphate solution was prepared using KH_2PO_4 with distilled water spiked with different concentrations (2–50 mg/L).

2.2 Preparation of Adsorbent

The zeolite ball coated with sulfate (ZBCS) was prepared by agglomeration with an acrylic binder. The prepared zeolite ball (ZB) was calcined for 3 h under 750 °C to increase the hardness. To make a synthesis of ZBCS, 100 g of ZB was immersed in 500 mL of 10 % sulfuric acid solution for 18 h. After the immersion process, to compare the degree of surface coating for the sulfate, the ZB immersed in sulfate solution was calcined in the two types of furnace: one is a gas furnace injected with mixed gas composed of 95 % nitrogen and 5 % hydrogen, and the other is an electric furnace. Both heating processes were maintained at 300 °C for 3 h. After the calcination, the ZBCS was cooled to room temperature and washed using distilled water with pH 7.0. Then, it was dried at 80 °C in an oven and stored in a desiccator.

2.3 Batch Adsorption Test

To determine the maximum adsorption capacities of the ZBCS, equilibrium batch tests were conducted. Five hundred milligrams of ZBCS was reacted with 200 mL of phosphate solution with various initial concentrations (2, 5, 10, 25, and 50 mg/L) in conical tubes using a rotator shaker (GTR-100, Digital Rotator, Green-Tech, Seoul, Korea). After the reaction reached an equilibrium (approximately 12 h), the samples became a supernatant in the tubes and were filtered through 0.45 μm syringe filters. The phosphate concentration was analyzed at the end.

The ZBCSs synthesized by the different furnace types were also prepared for kinetic batch tests. Fifty milligrams of ZBCSs was added to each 200 mL conical tube containing 50 mg/L of phosphate solution. At regular time intervals (10, 30, 60, 120, 240, 480, 720, and 1,440 min), liquid samples were withdrawn and the phosphate concentration was analyzed. The kinetic

batch tests were conducted for 24 h until the aqueous phosphate concentrations showed no changes.

2.4 Lab-Scale Column Test

The fixed bed reactor test was performed at the laboratory scale to evaluate the performance of the adsorbent. The breakthrough tests were conducted with a packed bed column with total length of 28 cm and inner diameter of 6 cm. The column container was a Pyrex tube. The column was packed with 0.99 kg of ZBCS. The ZBCS was added from the top of the column and allowed to settle down by gravity. A predetermined quantity of the ZBCS was packed in the column. Phosphate solutions of known concentration were injected upward through the column at a constant rate of 90 mL/min at room temperature using a controlled volume pump (Aquatech Asia Co. Ltd., Model BP-1000, Republic of Korea). The phosphate concentration in the effluent was monitored for 3 weeks and measured using ion chromatography. After the column adsorption test, the ZBCS was regenerated. To evaluate the performance of the regenerated adsorbent, the fixed bed reactor test was repeated three times using the regenerated ZBCS. Figure 1 shows the experimental setup that was used.

2.5 Pilot Plant Test

Based on the results of the lab-scale column test, a pilot-scale plant test was constructed at the Pangyo sewage treatment center. A detailed picture of the pilot plant is presented in Fig. 2: panel a shows the phosphate removal system installed in the Pangyo sewage treatment center and panel b shows part of the automatic measurement equipment for phosphate. As illustrated in Fig. 3, the pilot plant was comprised of a feed pump, a micro filter, the reactors, and the regenerant. These systems were fabricated by Hyflux Co. Ltd., and comprised a micro filter (30 L), a reactor (100 L), and a regenerant (70 L). The pilot plant system was connected at the secondary effluent from the sewage treatment plant and was equipped with a micro filter to prevent suspended solid particles from passing through the inlet. This filter is changed for a new one every third day. Fifty kilograms of ZBCS was packed in each reactor and a 5 % sulfuric acid solution was used as a chemical for regeneration of adsorbents. As shown in the Fig. 2b, the real-time measurement instrument for phosphate concentration was installed in this system and connected to a laptop computer for saving the data once every 50 min. The quantity of secondary effluent injected in this system was 72,000 L/day.

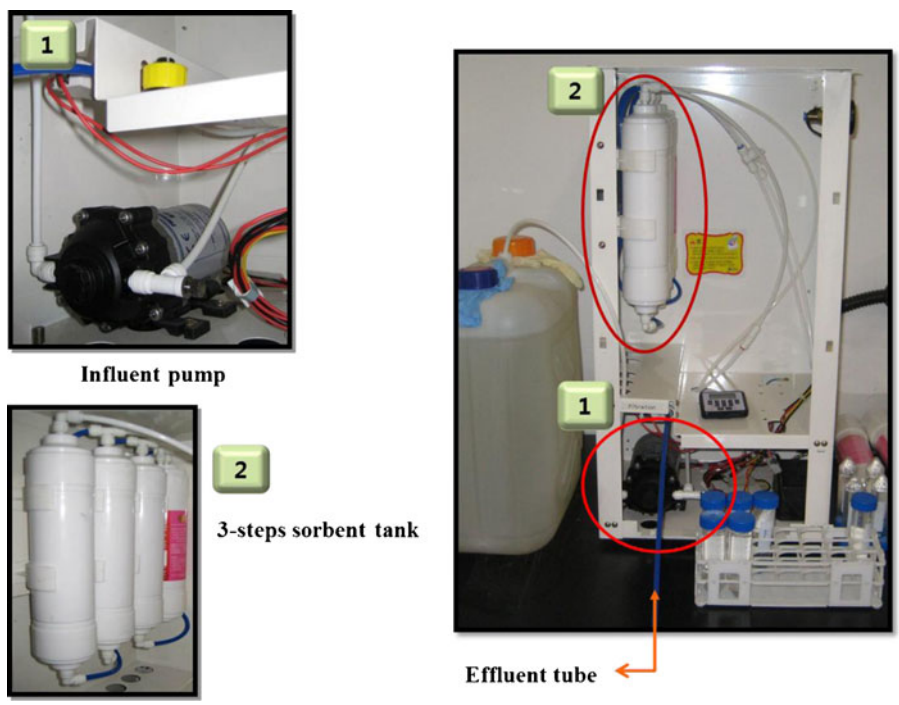

Fig. 1 Experimental apparatus for the lab-scale column test

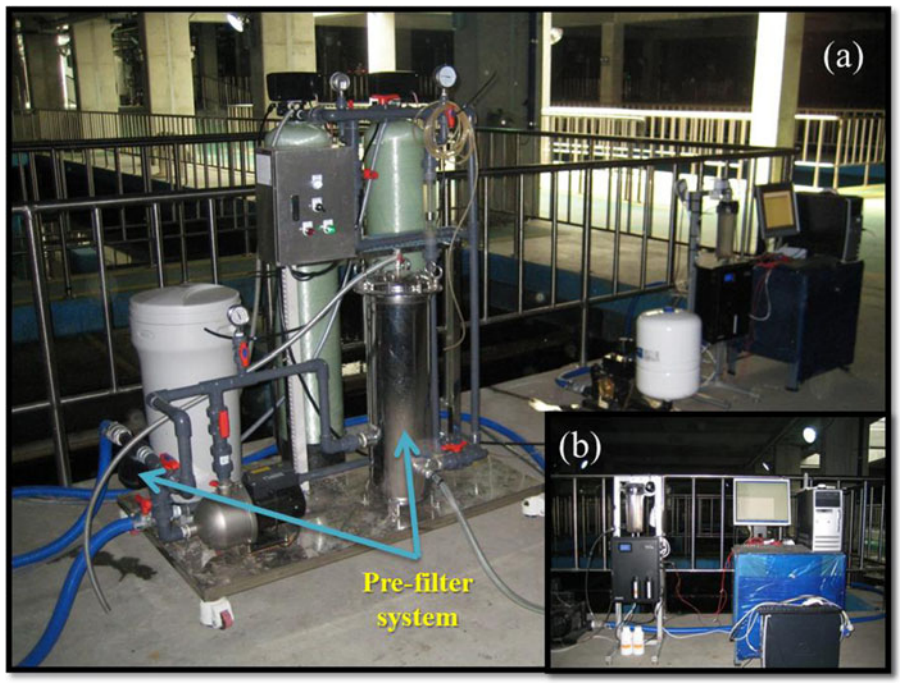

Fig. 2 **a** Site image of equipment in the pilot plant and **b** the automatic phosphate measurement system

2.6 Mathematical Modeling

2.6.1 Batch Adsorption Isotherm Modeling

To quantify the adsorption capacity for the ZBCS, equilibrium and kinetic adsorption models were used by following the Langmuir adsorption isotherm (Eq. (1)) and pseudo-first-order kinetic models (Eq. (2)) (Choi et al. 2011), as follows:

$$S = \frac{\alpha\beta C}{1 + \alpha C} \tag{1}$$

where S and C are the adsorbed and residual aqueous concentrations, and α and β are the constants related to the binding energy (in liter per milligram) and the maximum adsorption capacity (in milligram per kilogram), respectively.

$$\log(q_e - q_t) = \log(q_e) - \frac{k_1}{2.303} t \tag{2}$$

where k_1 is the rate constant of pseudo-first-order adsorption (1/min), q_e is the amount of phosphate sorbed at equilibrium (in milligram per gram) and q_t is the amount of phosphate sorbed at time t (in milligram per gram).

2.6.2 The Thomas Model

The Thomas model was employed to evaluate the adsorption capacity of the ZBCS in a column experiment (Thomas 1944). The expression for the Thomas model is given below (Eq. (3)):

$$\frac{C_t}{C_0} = \frac{1}{1 + \exp\left(\left(q_T M - C_0 F t\right)^{k_T/F}\right)} \tag{3}$$

where k_T is the Thomas rate constant (in milliliter per minute per milligram), q_0 is the theoretical saturated adsorption capacity in Thomas model (in milligram per gram), F is the flow rate of the effluent (in milliliter per minute), M is the mass of the adsorbent (in gram), C_0 is the influent phosphate concentration (in milligram per liter), and C_t is the effluent phosphate concentration at time t (in milligram per liter). The k_T and q_0 can be determined from a plot of C_t/C_0 against t at a given flow rate using nonlinear regression.

2.6.3 Mathematical Description

The value of q_{total} for a given feed concentration and flow rate is equal to the area under the plot of the adsorbed phosphate concentration $C_0 - C_t$ (in milligram per liter)

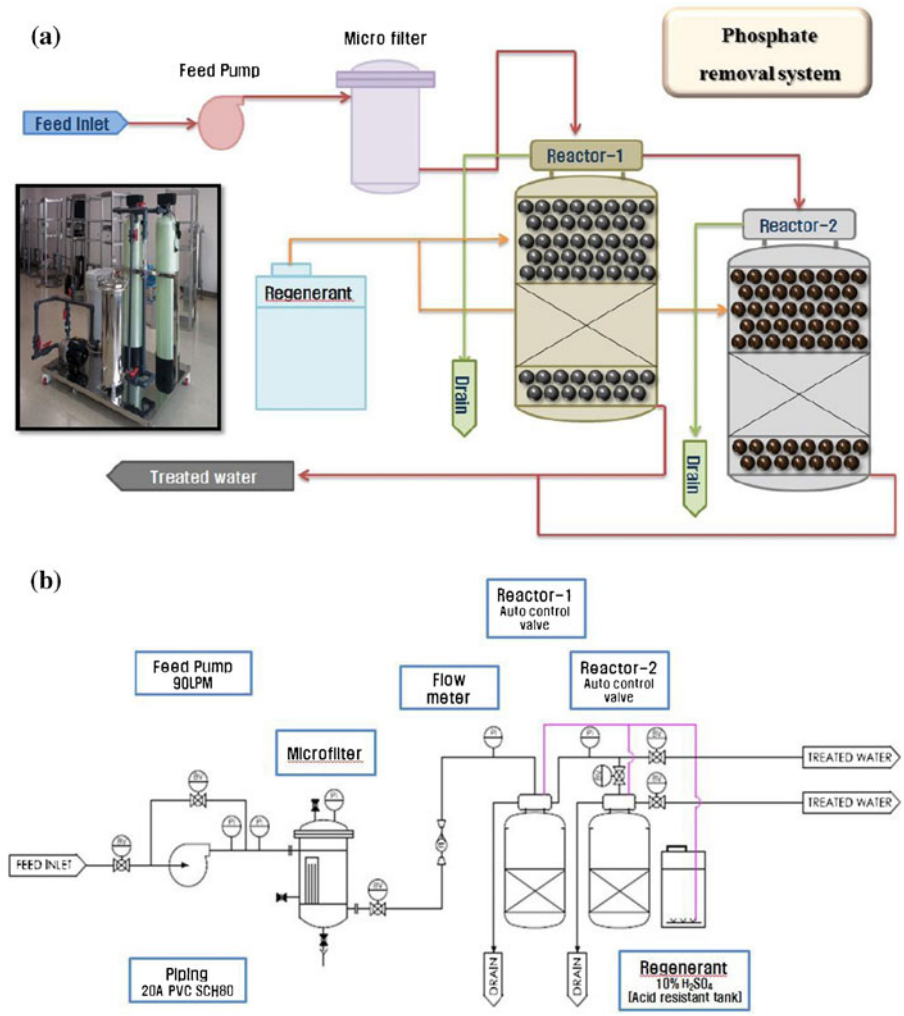

Fig. 3 **a** Schematic diagram and actual image and **b** detailed design figure for the pilot plant

vs. t (in minute) and calculated from the following equation (Han et al. 2009):

$$q_{total} = \int_0^{t_{total}} F(C_0 - C_t)dt \quad (4)$$

The value of $q_{e\ (exp)}$ is calculated as the following:

$$q_{e(exp)} = {}^{q_{total}}/_{M} \quad (5)$$

The total amount of phosphate injected into the reactor W_{total} (in milligram) is calculated from the following:

$$W_{total} = C_0\, F\, t_{total} \quad (6)$$

The total removal ratio of phosphate Y (in percent) is the ratio of the maximum capacity of the column (q_{total}) to the total amount of phosphate injected into the reactor (W_{total}).

$$Y = q_{total}/W_{total} \times 100 \quad (7)$$

2.7 Regeneration Experiments

After the column and pilot plant tests, the ZBCS was regenerated by the following procedure. In the case of the column experiment, a 5 % sulfuric acid solution was injected into the ZBCS-packed column at an equal flow rate in the column tests for 6 h. Next, distilled water was injected into the column to wash the remnants of sulfuric acid from inside the column. On the other hand, in the case of the pilot plant, a 5 % sulfuric acid solution in the regenerant was circulated throughout the column for regeneration of ZBCS and flowed back into the regenerant vessel. The increase in the number of times

being regenerated is the factor that can increase the phosphate to sulfate concentration ratio.

2.8 Analytical Methods

The specific surface area of the ZBCS was measured using a Brunauer–Emmett–Teller (BET) isotherm plot (Micromeritics Gemini 2375-CCR238, Georgia, USA). The surface morphology of the developed adsorbent was observed with a scanning electron microscope (SEM, LEO-1530VP, LEO Electron Microscopy Ltd, England). To observe the distribution of the sulfate element on the ZBCS, an electron probe microanalysis (EPMA, JEOL 8800R, USA) was performed both before and after the sulfate coating step. The SEM ISI DS-130 coupled to a SparcStation 5 for energy-dispersive X-ray (EDX) analysis was used to evaluate the chemical composition and the distribution of materials on the surface. The phosphate concentration was determined using an ion chromatograph (ICS-1000, DIONEX, USA).

3 Results and Discussion

3.1 Characteristics of the Surface-Modified Zeolite Ball (SEM, EPMA, EDX, and BET)

The actual and SEM photographs are shown in Fig. 4a–c. The SEM images were taken at 10,000 times magnification to observe the surface morphologies of the ZBCS. Figure 4a is the real size image of the ZBCS that can be manufactured with 2.0 ~ 10.0 mm diameters. If the diameter of the ZBCS is over 10.0 mm, the stability of the adsorbent and the phosphate removal efficiency are decreased due to the diminution of the hardness of the adsorbent and the specific surface area. The SEM images shown in panels b and c in Fig. 4 show the surface morphologies of the non-coated zeolite ball and sulfate-coated zeolite ball, respectively. The coated zeolite ball surface was apparently occupied by sulfate, which formed into clumps. After the sulfate coating, sulfate was deposited on the zeolite ball surface, clogging the cavities in the coating process. However, the micropores connected to the inside of the ZBCS were maintained,

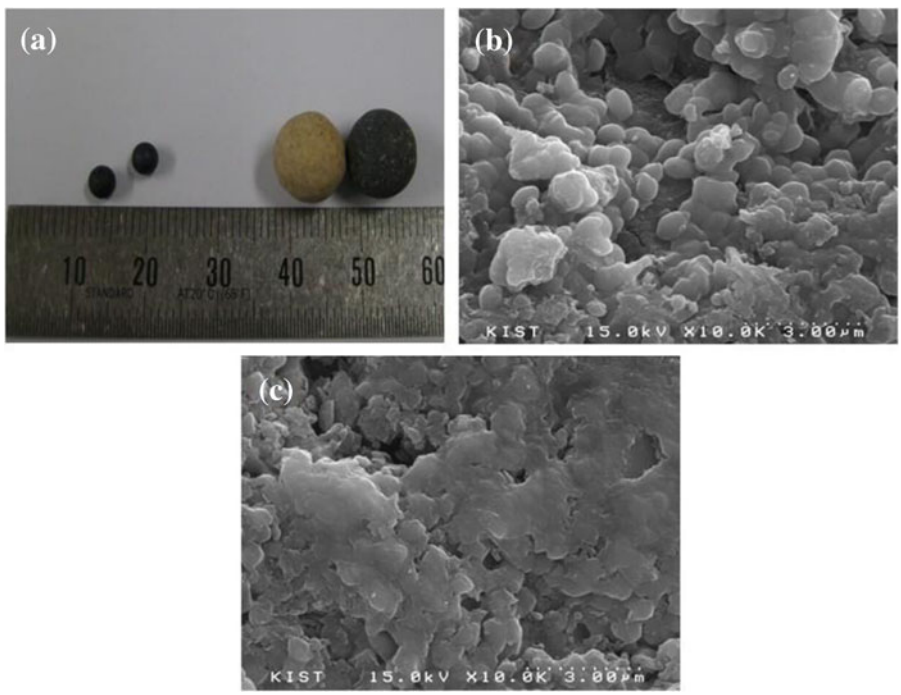

Fig. 4 **a** Actual zeolite ball images; **b** SEM images for the zeolite ball before; and **c** after surface modification

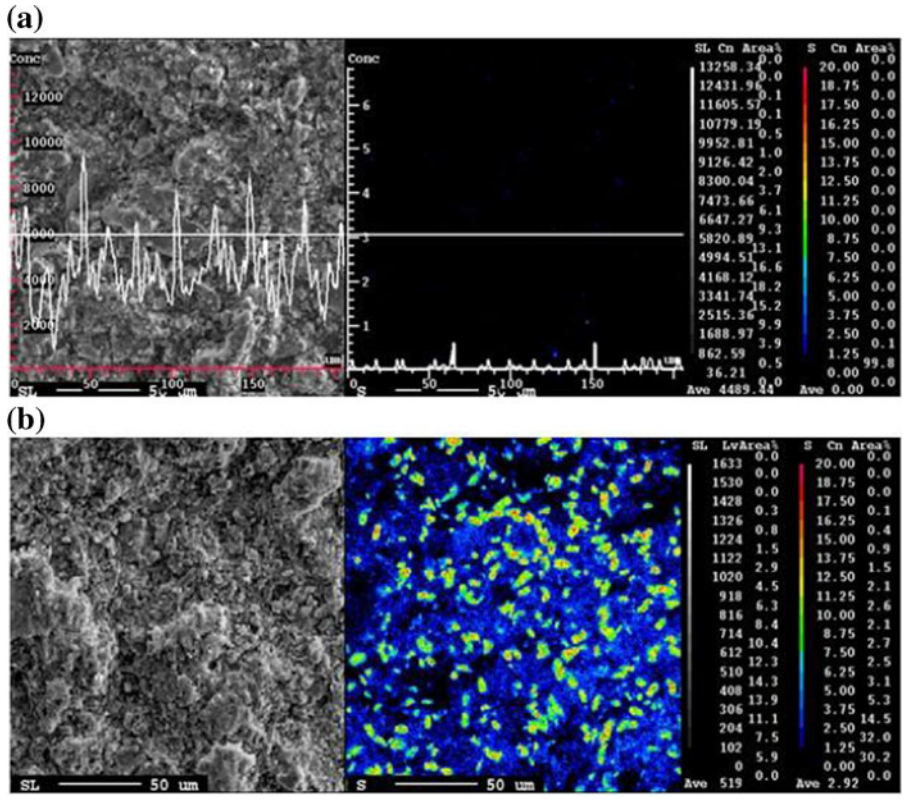

Fig. 5 EPMA element maps for sulfate: **a** the zeolite ball surface before modification with sulfate; **b** after modification with sulfate

which can remove phosphate through the zeolite ball surface as well as the micropores connected to the inside.

To investigate the distribution of the sulfate element during the calcination process and explain the observed

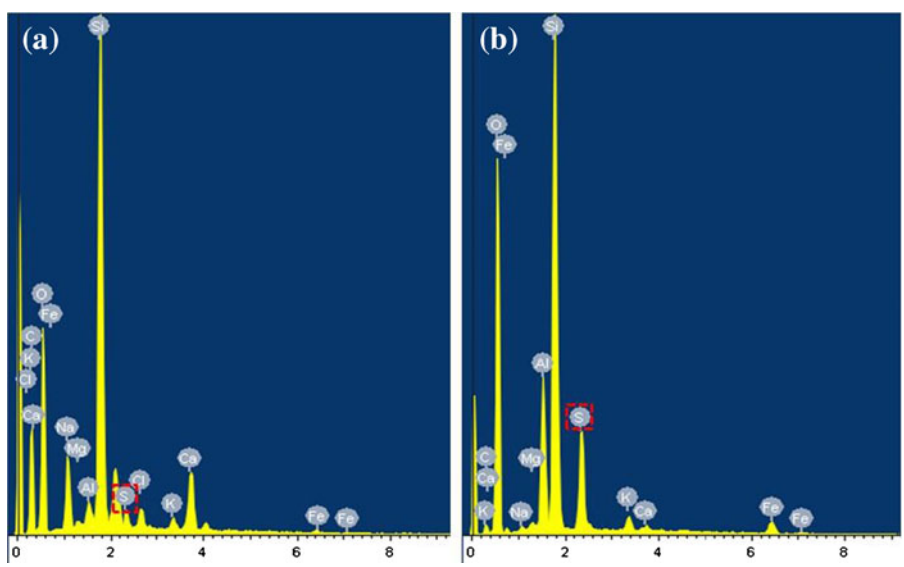

Fig. 6 EDX spectra for the zeolite ball surface **a** before modification with sulfate and **b** after modification with sulfate

Table 1 Characteristic parameters of sulfate coated zeolite before and after modification

Samples	S_{BET} (m^2/g)	D_P (nm)	V_P (cm^3/g)
Before modification	26.3477	24.872	0.100074
After modification	9.3831	14.822	0.058346

differences between the ZBCS and the non-coated zeolite surface, the EPMA mapping method was employed. Figure 5 shows the sulfate on the occupied zeolite ball surface. The non-coated zeolite surface shown in Fig. 5a has a black color without the sulfate coating; however, Fig. 5b displays the distribution of sulfate indicated by the uniform color index.

EDX data of the zeolite ball surface before and after coating with sulfate show the presence of silicate, iron, oxygen, carbon, and sodium (Fig. 6a, b). EDX data clearly indicate the increase in the sulfur peak and the decrease in the potassium and sodium peaks after the surface modification. Thus, adsorption of phosphate by ZBCS might proceed through an anion exchange mechanism. Therefore, it is proposed that the sulfate ion replaces phosphate in the aqueous phase through ionic interaction.

Table 1 summarizes the results of the nitrogen adsorption experiment (before and after surface modification), including BET surface area (S_{BET}), pore volume (V_P), and pore size (D_P) in the Barrett–Joyner–Halenda distributions. The surface areas before and after modification of the zeolite were calculated to be 26.3477 and 9.3831 m^2/g, respectively. The zeolite before the sulfate coating exhibited a large surface area; however, its surface area drastically decreased after the sulfate modification. In the case of the pore diameter and volume, similar trends are observed. Pore diameter and volume decrease significantly after the sulfate modification and these facts indicate that the sulfate functional group is distributed over a considerable portion of the zeolite surface. Therefore, the surface area, pore diameter, and pore volume decreased after the sulfate coated the zeolite surface. The decrease in the BET parameters for the sulfate-coated zeolite is attributed to the occupation of the pore framework by the sulfate functional group and the surface modification by the sulfate treatment.

3.2 Lab-Scale Batch Adsorption Tests

The adsorption isotherm data (Fig. 7) satisfactorily fitted to the Langmuir adsorption model (Table 2) and the value of the maximum adsorption capacities of the ZBCS calcined under inert (Gas furnace case 1 and 2) and oxidative (Electric furnace) conditions were 15.04, 15.13, and 3.66 mg/g, respectively. All of the isotherms resulted in a nonlinear curve with an asymptotic increase that fits the Langmuir adsorption isotherm model. The adsorption capacity of the ZBCS is among the highest values reported for other adsorbents in the literature (Table 2). The adsorption isotherm of ZBCS calcined under inert conditions showed a sharp increase of adsorbed concentration in the lower range of the equilibrium concentration;

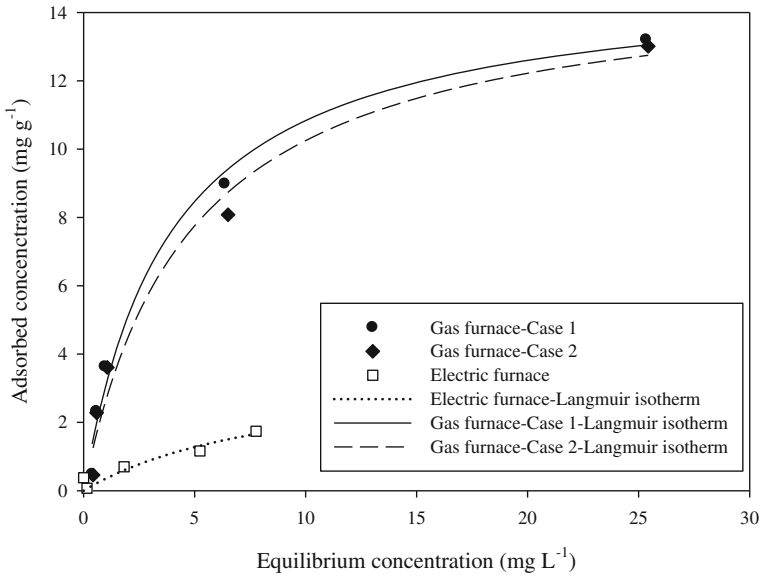

Fig. 7 Comparison of the adsorption capacities of the zeolite ball modified with sulfate under inert and oxidizing conditions

Table 2 Langmuir isotherm parameters for phosphate adsorption according to calcination conditions compared with various other adsorbents

Langmuir equation ($S=\alpha\beta C/(1+\alpha C)$)			
	β (mg/g)	α (L/mg)	R^2
Gas furnace—case 1	15.04	0.2572	0.9867
Gas furnace—case 2	15.13	0.2099	0.9785
Electric furnace	3.66	0.1071	0.9037
Activated carbon (Mahmudov and Huang 2011)	8.09	–	–
Iron and zirconium binary oxide (Long et al. 2011)	13.65	–	–
Bauxsol (Akhurst et al. 2006)	0.45	–	–
Purolite A500P (Gupta et al. 2012)	14.00	–	–
Iron oxide tailings (Zeng et al. 2004)	12.65	0.3690	0.9930

however, it reached maximum capacity at approximately 25 mg/L. This result indicates that the binding energy (α) of the ZBCS for phosphate seems to be high and the energy requirement for phosphate adsorption is low. The pH variation was decreased from 4.76 to 4.28 before and after phosphate reaction. However, it was not a significant change. In addition, the experimental data for the ZBCS fit the isotherm equation well, with correlation coefficients ranging from 0.90 to 0.99.

The adsorbed concentration of phosphate as a function of the reaction time is shown in Fig. 8. The related parameters, such as the adsorption constant values, the correlation coefficients, and the experimental and predicted q_e values for the pseudo-first-order kinetic model are shown in Table 3. The data show that the adsorption of phosphate onto the ZBCS calcined under inert conditions was fast, with equilibrium attained after 180 min. In the case of the ZBCS calcined under oxidative conditions, a little phosphate had been removed from the aqueous phase after the reaction. These results show that the sulfate coating on the zeolite ball functioned as a reactor when the zeolite ball was calcined under inert conditions and soaked in sulfate solution. Namely, the sulfate function was supported on the zeolite ball surface because the oxygen ions did not oxidize onto the surface of the base material under inert conditions. The overall results for the lab-scale batch adsorption test indicate that ZBCS may be useful as an adsorbent for the treatment of sewage containing phosphate anion.

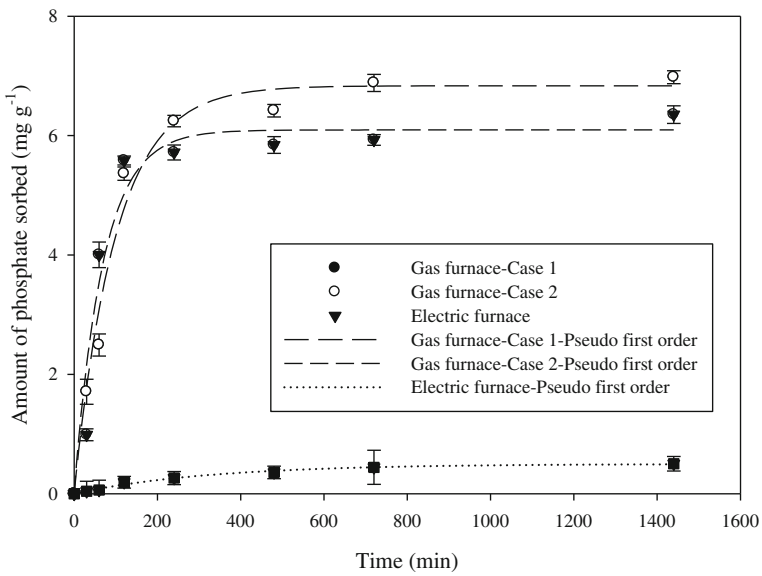

Fig. 8 Comparison of the kinetic adsorption for phosphate on the zeolite ball modified with sulfate under inert and oxidizing conditions

Table 3 Kinetic parameters for the adsorption of phosphate according to calcination condition

Pseudo-first-order model ($q_t=q_e(1-e^{-kt})$)				
	$q_{e\ exp}$ (mg/g)	k_1 (1/min)	$q_{e\ mod}$ (mg/g)	R^2
Gas furnace—case 1	6.9775	0.0100	6.8344	0.9834
Gas furnace—case 2	6.3525	0.0144	6.0945	0.9513
Electric furnace	0.5025	0.0030	0.4992	0.9890

3.3 Fixed Bed Column and Pilot Plant Test

The breakthrough curves (BTCs) in the lab-scale test are shown in Fig. 9. The BTCs of pure ZBCS (lab 1) showed a faster breakthrough than those of the once- and twice-regenerated ZBCSs (labs 2 and 3), but a slower breakthrough than the thrice-regenerated ZBCSs (lab 4). As the regeneration of the ZBCS repeated, the breakthrough time becomes slightly faster. The BTCs in the field-scale test are shown in Fig. 10. Similar to the lab-scale test, the BTCs of the pure ZBCSs (field 1) broke through faster than those of the once- and twice-regenerated ZBCSs (fields 2 and 3). The breakthrough time of the twice-regenerated ZBCSs (field 3) is faster than that of the first regeneration (field 2).

The BTCs were fitted using the Thomas model. The resulting parameters are presented in Table 4. In the lab-scale test, the adsorption capacity (1.20 mg/g of q_e) of the pure ZBCS was much smaller than the β of the Langmuir isotherm (15.04~15.13 mg/g) and the $q_{e(exp)}$ (6.3525~6.9775 mg/g) of the kinetic parameter. Tests using the regenerated adsorbents (labs 2, 3, and 4) showed similar values of q_e and k_T compared to the values of the pure adsorbent (lab 1). This indicates that the regenerated ZBCS could maintain the adsorption property through the regeneration process. The efficiency of the regeneration process was confirmed by the field test. In the field test, the adsorption capacity (q_e) and rate (k_T) maintained similar values after regeneration. Although the values of q_e in the lab-scale test were smaller than that of the isotherm, the values of q_e in the field test were higher and thus similar to that of the adsorption isotherm. This might be due to suspended substances in the influent sewage. Because the lab-scale column test was conducted without removal of suspended solids in the sewage, part of the suspended solids covered the sorption sites on the ZBCS. However, in the pilot plant process, the filtration step was equipped for removal of suspended solid before inflow into the adsorption reactor. These results indicate that the filtration step was effective in the removal of inhibitory factors with the adsorption of phosphate. By the first regeneration, the values of q_e were commonly increased in the lab- and field tests. This might be due to the cleansing process during the regeneration procedure enhancing the adsorption capacity by securing

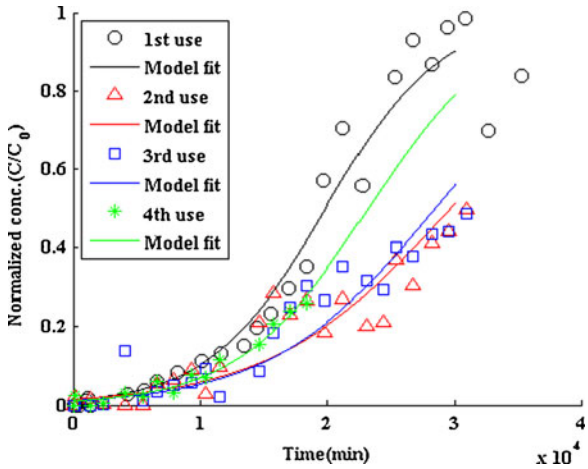

Fig. 9 Breakthrough curves from the lab-scale column condition: the effect of adsorbent regeneration (Thomas model)

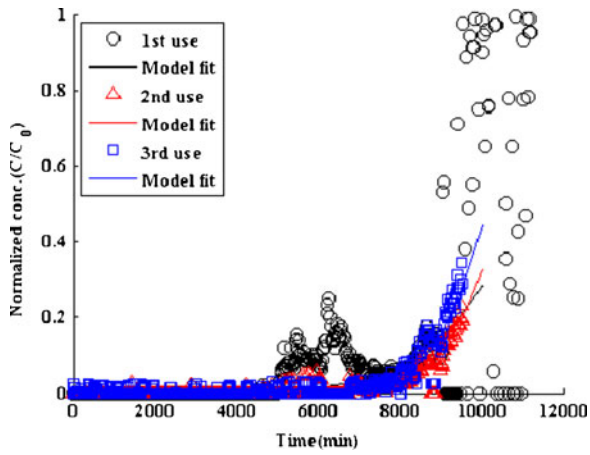

Fig. 10 Breakthrough curves from the pilot plant condition: the effect of adsorbent regeneration (Thomas model)

Table 4 Parameters of the Thomas model (k_T and q_e), the adsorption capacity from the experiment ($q_{e(exp)}$), and the total removal percent of phosphate (Y)

Exp.	M (g)	F (1/min)	C_0 (mg/L)	k_T (1/mg/min)	q_e (mg/g)	$q_{e(exp)}$ (mg/g)	Y (%)	C_0F/M[a]	C_0k_T[b] (1/min)
Lab 1	9.9E+02	9.0E−02	6.7E−01	3.3E−04	1.2E+00	1.2E+00	5.6E+01	6.1E−05	2.2E−04
Lab 2	9.9E+02	9.0E−02	4.5E−01	3.2E−04	1.2E+00	1.0E+00	8.2E+01	4.1E−05	1.4E−04
Lab 3	9.9E+02	9.0E−02	4.4E−01	3.6E−04	1.1E+00	9.9E−01	8.1E+01	4.0E−05	1.6E−04
Lab 4	9.9E+02	9.0E−02	4.0E−01	4.9E−04	8.5E−01	6.1E−01	9.1E+01	3.7E−05	2.0E−04
Field1	5.0E+04	5.0E+01	7.9E−01	1.0E−03	8.8E+00	7.2E+00	8.2E+01	7.9E−04	8.1E−04
Field2	5.0E+04	5.0E+01	1.2E+00	1.2E−03	1.3E+01	1.1E+01	9.8E+01	1.2E−03	1.4E−03
Field3	5.0E+04	5.0E+01	8.7E−01	1.7E−03	8.9E+00	8.8E+00	9.7E+01	8.7E−04	1.5E−03

[a] Phosphate flux per unit of adsorbent

[b] Rate of phosphate removal

additional sorption sites on the ZBCS. The values of q_e gradually decrease with repeated regeneration processes.

The adsorption rate (k_T) in the field tests was higher than the rate in the lab-scale test due to the increase in the adsorption flux per unit of adsorbent ($C_0\,F/M$). This result indicates that the adsorption processes in the lab column and the field reactor were limited by the slow flow rate. The rate of phosphate removal ($C_0\,k_T$) is much smaller than the values of k_1 in the kinetic batch test, indicating that the ZBCS could be efficiently operated with a much higher flow rate.

3.4 Proposal for Efficient Regeneration of ZBCS and Phosphate Recovery

The adsorption of phosphate in the aqueous phase causes the release of a sulfate ion on the ZBCS surface. After the adsorption reaction with the phosphate, the spent ZBCS is not reusable. To reactivate the function of the ZBCS, it can be regenerated by a reaction with a 10 % sulfuric acid solution as in the preparation process of the adsorbent. However, the calcination step is excluded from the regeneration process of ZBCS. Because the sulfate already formed a chemical functional group on the ZBCS, surface calcination is not needed for regeneration. Sections 3.3 and 3.4 showed that the regeneration of ZBCS was effective in the column experiment at lab scale and in the pilot plant test. These results ensure that the synthesized adsorbent in this study is commercially available for the sewage treatment facilities.

In addition, the regeneration solution used for recycling the ZBCS in the pilot plant is enriched with sulfate ion. The enriched solution could be used in resource recovery by various methods. In the best example, a mineral type such as struvite can be recovered. The recovered struvite does not contain hazardous compounds and has been characterized as more effective as fertilizer than conventional chemical fertilizers. Additionally, it does not require an industrial precipitation process for products such as detergents, cosmetics, and animal feed (de-Bashan and Bashan 2004). Meanwhile, there is an additional use as anti-scales. Anti-scales are chemicals that are used for prevention of scale and corrosion in pipe conduits in boilers and heat exchangers. Phosphate is a key ingredient in the anti-scales. An important functional property of phosphate is that it contributes to the overall detergency of anti-scales by providing and controlling alkalinity. The control of the proper pH can assist in the removal of fatty compounds, protect against corrosion, and prevent the re-deposition of scales on the inside wall of the pipe conduit. The enriched regeneration solution might be used as an anti-scale agent if the phosphate concentration is adjusted.

4 Conclusions

The results of various adsorption tests, such as batch, column, and pilot plant, showed that the ZBCS is a potential adsorbent for treatment of phosphate from sewage and wastewater. Of the two ZBCSs calcined under inert and oxidative conditions tested in the batch study, the inert condition had the highest phosphate removal capacity. The kinetics of phosphate adsorption by ZBCS in the batch study was satisfactorily described by a pseudo-first-order model. The empirical Thomas model

also appropriately described the phosphate adsorption behavior in a fixed-bed column and in the packed ZBCS in the pilot plant. The experimental breakthrough adsorption capacities matched the prediction of the Thomas model well. However, the maximum adsorption capacity calculated from the equilibrium batch test was higher than these of the column and the pilot plant. The phosphate removed through the adsorption process was condensed in the regeneration solution. The condensed phosphate could be recovered for resources such as struvite through a reaction with magnesium. The high quality of the obtained struvite by the recovery process indicates that minimum steps are required before reuse. The regeneration solution could be also directly used if the concentration of phosphate was adequately adjusted. The results of these studies indicate that ZBCS is an effective and inexpensive adsorbent for phosphate removal and recovery from the aqueous phase.

Acknowledgments This research is supported by a grant from the Korea Ministry of Environment as "Global Top Project" (GT-11-B-01-011-1) and the Korea Institute of Science and Technology (KIST) institutional program (2E23943).

References

Aguado, J., Arsuaga, J. M., Arencibia, A., Lindo, M., & Gascón, V. (2009). Aqueous heavy metals removal by adsorption on amine-functionalized mesoporous silica. *Journal of Hazardous Materials, 163*(1), 213–221.

Akhurst, D. J., Jones, G. B., Clark, M., & McConchie, D. (2006). Phosphate removal from aqueous solutions using neutralized bauxite refinery residues (Bauxsol^{TM}). *Environmental Chemistry, 3*, 65–74.

Benyoucef, S., & Amrani, M. (2011). Adsorption of phosphate ions onto low cost Aleppo pine adsorbent. *Desalination, 275*, 231–236.

Blaney, L. M., Cinar, S., & Sengupta, A. K. (2007). Hybrid anion exchanger for trace phosphate removal from water and wastewater. *Water Research, 41*, 1603–1613.

Boyer, T. H., Persaud, A., Banerjee, P., & Palomino, P. (2011). Comparison of low-cost and engineered materials for phosphorus removal from organic-rich surface water. *Water Research, 45*, 4803–4814.

Celik, F. E., Kim, T. J., & Bell, A. T. (2010). Effect of zeolite framework type and Si/Al ratio on dimethoxymethane carbonylation. *Journal of Catalysis, 270*, 185–195.

Choi, J. W., Lee, S. Y., Chung, S. G., Hong, S. W., Kim, D. J., & Lee, S. H. (2011). Removal of phosphate from aqueous solution by functionalized mesoporous materials. *Water, Air, and Soil Pollution, 222*, 243–254.

Choi, J. W., Lee, S. Y., Lee, S. H., Lee, K. B., Kim, D. J., & Hong, S. W. (2012). Adsorption of phosphate by amino-functionalized and co-condensed SBA-15. *Water, Air, and Soil Pollution, 223*, 2551–2562.

de-Bashan, L. E., & Bashan, Y. (2004). Recent advances in removing phosphorus from wastewater and its future use as fertilizer (1997–2003). *Water Research, 38*, 4222–4246.

Dionisiou, N. S., Matsi, T., & Misopolinos, N. D. (2013). Phosphorus adsorption-desorption on a surfactant-modified natural zeolite: a laboratory study. *Water, Air, and Soil Pollution, 224*, 1362.

Felice, V., Ntais, S., & Tavares, A. C. (2013). Propyl sulfonic acid functionalization of faujasite-type zeolites: effect on water and methanol sorption and on proton conductivity. *Microporous and Mesoporous Materials, 169*, 128–136.

Gupta, M. D., Loganathan, P., & Vigneswaran, S. (2012). Adsorptive removal of nitrate and phosphate from water by a Purolite ion exchange resin and hydrous ferric oxide columns in series. *Separation Science and Technology, 47*(12), 1785–1792.

Han, R., Wang, Y., Zhao, X., Wang, Y., Xie, F., Cheng, J., et al. (2009). Adsorption of methylene blue by phoenix tree leaf powder in a fixed-bed column: experiments and prediction of breakthrough curves. *Desalination, 245*, 284–297.

Jiang, J. Q., & Graham, N. J. D. (1998). Pre-polymerised inorganic coagulants and phosphorus removal by coagulation—a review. *Water SA, 24*, 237–244.

Kandah, M. L. (2004). Zinc and cadmium adsorption on low-grade phosphate. *Separation and Purification Technology, 35*, 61–70.

Kim, Y. S., Lee, Y. H., An, B., Choi, S. A., Park, J. H., Jurng, J. S., et al. (2012). Simultaneous removal of phosphate and nitrate in wastewater using high-capacity anion-exchange resin. *Water, Air, and Soil Pollution, 223*, 5959–5966.

Li, J., Xing, X. H., & Wang, B. Z. (2003). Characteristics of phosphorous removal from wastewater by biofilm sequencing batch reactor (SBR). *Biochemical Engineering Journal, 16*, 279–285.

Liang, X., Xu, Y., Wang, L., Sun, Y., Lin, D., Sun, Y., et al. (2013). Sorption of Pb^{2+} on mercapto functionalized sepiolite. *Chemosphere, 90*, 548–555.

Long, F., Gong, J. L., Zeng, G. M., Chen, L., Wang, X. Y., Deng, J. H., et al. (2011). Removal of phosphate from aqueous solution by magnetic Fe-Zr binary oxide. *Chemical Engineering Journal, 171*, 448–455.

Low, L. W., Teng, T. T., Ahmad, A., Morad, N., & Wong, Y. S. (2011). A novel pretreatment method of linocellulosic material as adsorbent and kinetic study of dye waste adsorption. *Water, Air, and Soil Pollution, 218*, 293–306.

Mahmudov, R., & Huang, C. P. (2011). Selective adsorption of oxyanions on activated carbon exemplified by Filtrasorb400 (F400). *Separation and Purification Technology, 77*, 294–300.

Mohammed, F. M., Roberts, E. P. L., Hill, A., Campen, A. K., & Brown, N. W. (2011). Continuous water treatment by adsorption and electrochemical regeneration. *Water Research, 45*, 3065–3074.

Motsa, M. M., Thwala, J. M., Msagati, T. A. M., & Mamba, B. B. (2012). Adsorption of 2,4,6-trichlorophenol and *ortho*-nitrophenol from aqueous media using surfactant-modified clinoptilolite-polypropylene hollow fibre composites. *Water, Air, and Soil Pollution, 223*, 1555–1569.

Oehmen, A., Lemos, P. C., Carbalho, G., Yuan, Z. G., Keller, J., Blackall, L. L., et al. (2007). Advances in enhanced biological phosphorus removal: from micro to macro scale. *Water Research, 41*, 2271–2300.

Ozacar, M. (2003). Adsorption of phosphate from aqueous solution onto alunite. *Chemosphere, 51*, 321–327.

Simmons, J. A. (2010). Phosphorus removal by sediment in streams contaminated with acid mine drainage. *Water, Air, and Soil Pollution, 209*, 123–132.

Thomas, H. C. (1944). Heterogeneous ion exchange in a flowing system. *Journal of the American Chemical Society, 66*, 1664–1666.

Tillman, F. D., Bartelt-Hunt, S. L., Craver, V. A., Smith, J. A., & Alther, G. R. (2005). Relative metal ion sorption on natural and engineered sorbents: batch and column studies. *Environmental Engineering Science, 22*, 400–409.

Zaib, Q., Khan, I. A., Saleh, N. B., Flora, J. R. V., Park, Y. G., & Yoon, Y. (2012). Removal of bisphenol A and 17β-estradiol by single-walled carbon nanotubes in aqueous solution: adsorption and molecular modeling. *Water, Air, and Soil Pollution, 223*, 3281–3293.

Zeng, L., Li, X., & Liu, J. (2004). Adsorptive removal of phosphate from aqueous solutions using iron oxide tailings. *Water Research, 38*, 1318–1326.